Environ Earth Sci (2016) 75:872
DOI 10.1007/s12665-016-5616-3

ORIGINAL ARTICLE

Divisions based on groundwater chemical characteristics and discrimination of water inrush sources in the Pingdingshan coalfield

Xinyi Wang[1,2,3] · Hongying Ji[1] · Qi Wang[4] · Xiaoman Liu[1] · Dan Huang[5] · Xiaoping Yao[6] · Guoshen Chen[2]

Received: 8 February 2015 / Accepted: 7 April 2016 / Published online: 11 May 2016

Abstract Within the Pingdingshan coalfield, the spatial distribution characteristics of key groundwater chemical components were studied in four aquifers that influence coal-mining operations. Thirty-six water samples were collected from the four aquifers, which were divided into smaller units. Discriminant models of mine-water inrush sources were developed for the three divisions I, II_I, and II_{II}, and engineering verification was conducted. The results showed that the main indices influencing groundwater chemical characteristics were Na^++K^+, Ca^{2+}, Mg^{2+}, Cl^-, $SO_4{}^{2-}$, and HCO^{3-} in the Pingdingshan coalfield with regional variations according to faults and synclines. The Guodishan fault was the primary groundwater chemical division structure, which divides the Pingdingshan coalfield into two primary groundwater chemically characteristic units, divisions I and II. The Likou syncline was the secondary groundwater chemically characteristic structure, which divides division II into two secondary groundwater chemically characteristic units: divisions II_I and II_{II}. Discriminant models of water inrush sources in divisions I, II_I, and II_{II} (12 discriminant functions) were developed, and engineering verification showed that discrimination accuracy for 16 groundwater samples in four aquifers of three divisions was 93.75 %.

Keywords Geological characteristics · Key groundwater chemical components · Distribution law · Detail division · Water inrush source · Discriminant models

Introduction

Water disasters are a serious threat to mining safety. Finding water inrush sources and approaches is the basis of water disaster control, and discriminating water inrush sources accurately is a prerequisite for finding water inrush approaches. The study of element sources and transport in subterranean waters in different geological environments combines the disciplines of water chemistry and hydrogeology (Wang et al. 2012; Huang et al. 2012; Masaoki et al. 2014; Rajesh et al. 2012; Frondini et al. 2014; Srinivasamoorthy et al. 2014; Kuldip et al. 2011; Chidambaram et al. 2013). Recently, discriminating water inrush sources based on chemical characteristics has been a research focus using both quantitative and semi-quantitative methods (Clemens et al. 2002; Zhuk and Serikova 2005; Li 2008; Huang and Chen 2011a, b; Wang et al. 2011; Zhou et al. 2010). Discriminant models have been widely used for identifying water inrush sources, but the accuracy decreases in complex hydrogeological coalfields (Vittecoq et al. 2014; Lavoie et al. 2014; Lahcen et al. 2004), and thus the pertinence and effectiveness of water inrush prevention and control strategies reduce. Based on coalfield geological characteristics, every aquifer influencing coal-mining

✉ Hongying Ji
jihongying321@163.com

1 Institute of Resources and Environment, Henan Polytechnic University, Jiaozuo, Henan, China

2 China Pingmei Shenma Group, Pingdingshan, Henan, China

3 Collaborative Innovation Center of Coalbed Methane and Shale Gas for Central Plains Economic Region of Henan Province, Jiaozuo, Henan, China

4 College of Earth Science, University of Chinese Academy of Science, Beijing, 100049, China

5 Chongqing Nengke Engineering Exploration Co., LTD, Chongqing, China

6 School of Civil Engineering, Henan Polytechnic University, Jiaozuo, Henan, China

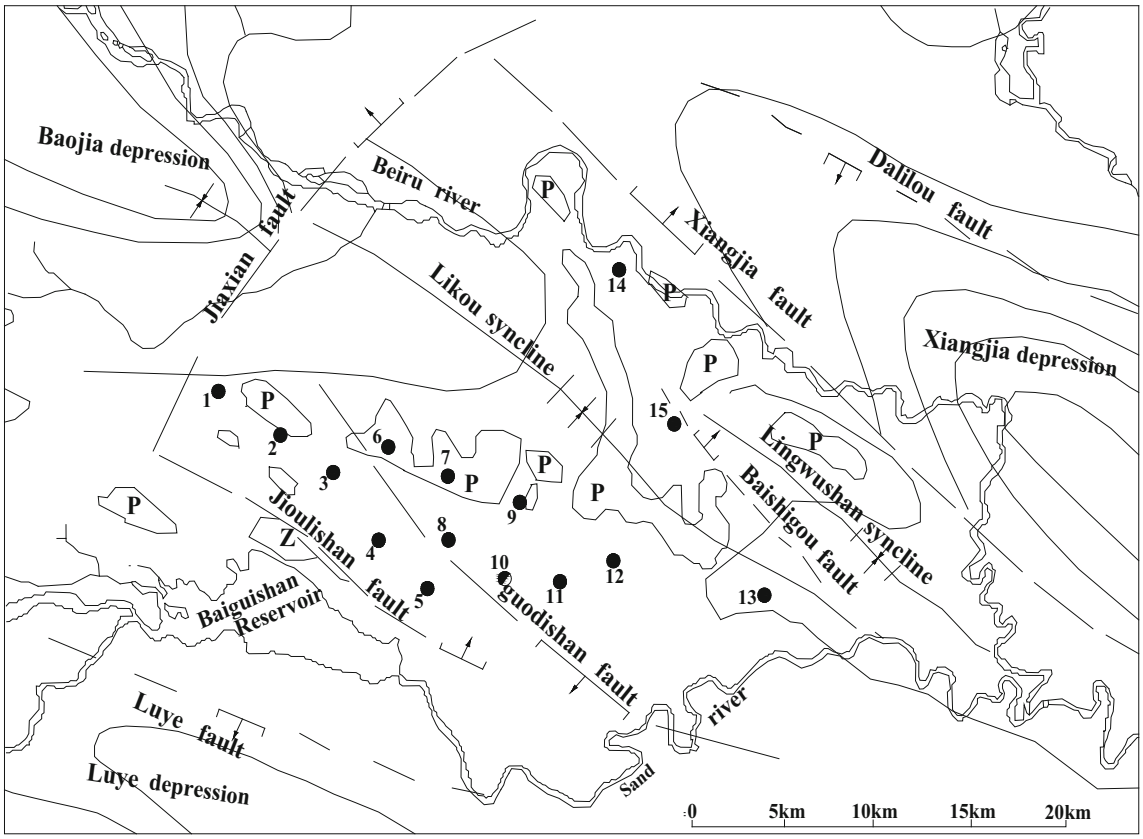

Fig. 1 Structural outline map of the Pingdingshan coalfield. *Numbers* show mine area, *1* was the Xiangshan mine, *2* the eleventh mine, *3* the ninth mine, *4* the fifth mine, *5* the seventh mine, *6* the sixth mine, *7* the fourth mine, *8* the third mine, *9* the first mine, *10* the second mine, *11* the tenth mine or Wuzhai mine, *12* the twelfth mine, *13* the eighth mine, *14* the thirteenth mine, and *15* the Shoushan mine. *P* was Permian, and *Z* profile

Table 1 Permian water-quality indices for the western part of the Guodishan fault (units: mg/L)

	K^++Na^+	Ca^{2+}	Mg^{2+}	Cl^-	SO_4^{2-}	HCO_3^-	Total hardness	Permanent hardness	Temporary hardness	Total alkalinity	Salinity	pH
1	809.60	4.80	15.07	151.02	143.12	1796.42	74.00	0.00	74.00	1472.00	2920.03	8.30
2	1109.73	15.63	8.88	94.66	24.98	2498.77	26.95	0.00	26.95	830.82	3923.80	8.40
3	1036.85	10.42	1.22	64.17	4.80	2288.25	31.03	0.00	31.03	2176.87	3614.37	8.40
4	284.16	13.03	7.05	31.56	4.94	768.84	61.58	0.00	61.58	630.60	1109.58	7.80
5	321.34	3.80	1.38	81.52	21.13	599.42	15.53	0.00	15.53	575.95	1080.37	8.10
6	68.31	57.72	23.35	18.08	94.14	329.50	239.88	0.00	239.88	269.86	592.50	7.50
7	158.24	167.13	173.4	30.49	1335.23	52.48	1129.42	1085.52	43.90	43.01	1917.53	6.30
8	31.27	76.35	11.07	21.27	46.50	277.03	237.74	10.53	227.21	227.21	464.09	7.80
9	14.02	76.18	12.64	19.01	40.33	248.96	242.20	38.02	204.18	204.18	411.14	7.40
10	14.25	73.21	13.98	18.53	39.09	249.57	240.23	35.52	204.72	204.72	411.63	7.50

operations were divided into smaller sections according to chemical distribution. Then, a water inrush source discriminant model was developed for every division and was found to have strong pertinence and high discriminant accuracy.

According to hydrogeological conditions in the Pingdingshan coalfield, this study analyzed the groundwater chemical characteristics of four aquifers influencing mining activities, determined their key groundwater chemical components, divided the four aquifers into key chemical component divisions by analyzing 36 groundwater samples, constructed a three-division discriminant model of water inrush sources, and performed engineering verification using 16 test samples. The results

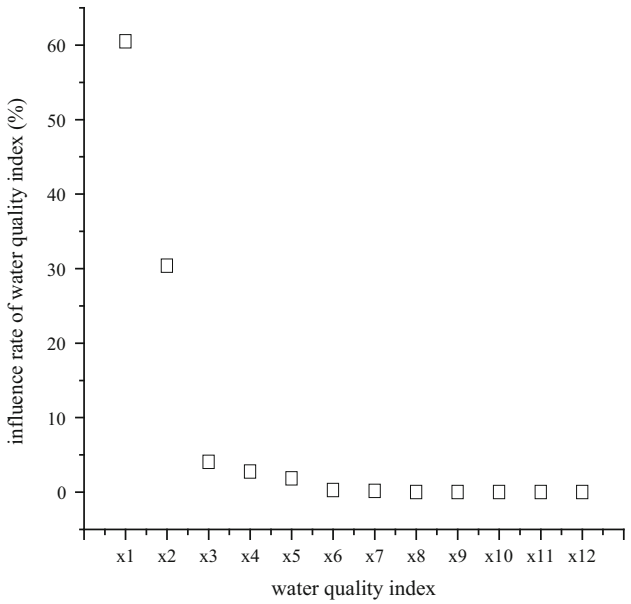

Fig. 2 Groundwater-quality index weights for the Pingdingshan coalfield. Na^++K^+, Ca^{2+}, Mg^{2+}, Cl^-, $SO_4{}^{2-}$, $HCO_3{}^-$, total hardness, permanent hardness, temporary hardness, total alkalinity, salinity, and pH were, respectively, defined as variables x_1, x_2, x_3, x_4, x_5, x_6, x_7, x_8, x_9, x_{10}, x_{11}, and x_{12}

provide a reference for correct discrimination of water inrush sources.

General Situation

The Pingdingshan coalfield is located in the eastern extension of a latitudinal structural zone in the Qinling Mountains and an E-type reflex arc top in the northwest wing of Huanyang Mountain. This area is a complex of latitudinal and E-type structures and forms a series of northwest compound folds in which main northwest tension–torsion and compression–torsion faults and secondary northeast tension–torsion faults control the coalfield structure. At present, the Xiangshan mine and the first through twelfth mines are located in the shallow south to Likou syncline, with the thirteenth mine and the Shoushan mine in the north to Likou syncline. The Guodishan fault forms a natural boundary between the third, fourth, and sixth mines and the seventh, ninth, and eleventh mines (Fig. 1).

The main mining seams in the Pingdingshan coalfield are the Taiyuan formation of the Carboniferous and the Shanxi and Xiashihezi formations of the Permian. The main aquifers influencing mining are composed of upper-middle thick Cambrian limestone, thin Taiyuan formation carboniferous limestone, Permian sandstone, and Quaternary gravel (Wang and Li 1992). Upper Middle Cambrian and Taiyuan formation carboniferous limestone aquifers are both direct and indirect water-filling sources of the Ji mining seam. Recharge conditions of Permian sandstone aquifers are worse because they are recharged by loose sand-gravel pore water at the bottom of the Quaternary and fissure weathering water through outcrops, and the degree of water penetration appears to show regional discrepancies due to fractures and faults. Sand-gravel Quaternary aquifers are recharged by precipitation and surface water, and their degree of water penetration is more affected by mining and the seasons.

The southwestern portion of the coalfield is a recharge area, whereas the eastern portion is a runoff area, and runoff is slow. The Cambrian and Carboniferous aquifers accept surface water infiltration directly or indirectly from the Quaternary and Permian and form a runoff trend from southwest to northeast. Before large-scale mining in the Pingdingshan coalfield, natural groundwater discharge was the main runoff mechanism. With increases in mining scale, long groundwater discharges form hydrophobic drop funnels around every mine, which compound each other from east to west, forming a long narrow shape from northwest to southeast, and have become the principal means of groundwater discharge from the mine area.

Component selection

Underwater chemistry is complex due to the occurrence environment, geological structure, and recharge conditions (Jin et al. 2001; Alexander et al. 2009; Pierre et al. 2014; Soren et al. 2008). Accurate selection of key groundwater chemical components is a prerequisite for dividing up the hydrogeological units and constructing discriminant models of water inrush sources.

Recharge water sources directly affect groundwater chemical components and, therefore, sample points for determining key chemical components should be located in groundwater recharge areas. The main aquifer recharge area is located in a bare Neogene limestone zone in the southwestern part of the Guodishan fault and, therefore, Permian samples from this area can serve to represent and analyze key groundwater chemical components in the Pingdingshan coalfield.

Using 10 groundwater samples from the ninth, fifth, and seventh mines, 12 water-quality indices, including Na^++K^+, Ca^{2+}, Mg^{2+}, Cl^-, $SO_4{}^{2-}$, $HCO_3{}^-$, total hardness, permanent hardness, temporary hardness, total alkalinity, salinity, and pH, were monitored (Table 1). The weights of these 12 water-quality indices were analyzed using the SPSS statistical software, and the resulting groundwater-quality index weights are shown in Fig. 2.

Figure 2 shows that the main groundwater-quality indices are the first six chemical components in the water,

Table 2 Analytical data for 25 samples on key groundwater chemical components

Aquifer	Mine	No.	Coordinate		K^++Na^+	Ca^{2+}	Mg^{2+}	Cl^-	SO_4^{2-}	HCO_3^-
			X	*Y*	(mg/L)	(mg/L)	(mg/L)	(mg/L)	(mg/L)	(mg/L)
Quaternary	Ninth	3	38,425,484	3,741,341	100.97	114.63	16.65	64.52	310.75	194.65
	Seventh	5	38,430,608	3,736,734	52.9	201.8	24.18	62.39	298.75	389.31
	Sixth	6	38,429,816	3,742,702	50.83	216.83	30.25	136.84	196.92	461.31
	Tenth	11	38,439,494	3,738,439	19.78	176.95	22.72	52.47	227.18	326.46
	Thirteenth	14	38,442,571	3,750,766	11.15	122.24	27.76	48.11	46.18	391.33
	Shoushan	15	38,445,834	3,743,743	14.49	171.94	10.57	70.55	119.59	341.71
Permian	Ninth	3	38,425,484	3,741,341	809.6	4.8	15.07	151.02	143.12	1796.42
	Fifth	4	38,428,890	3,740,353	1073.29	13.03	5.05	79.415	14.89	2393.51
	Seventh	5	38,430,608	3,736,734	224.60	24.85	10.59	43.72	40.07	565.92
	Sixth	6	38,429,816	3,742,702	600.28	7.28	12.15	101.82	86.92	1162.06
	Forth	7	38,432,077	3,740,188	35.19	79.62	24.69	26.83	58.18	328.18
	Thirteenth	14	38,442,571	3,750,766	391.13	16.8	10.33	54.137	178.50	671.14
Carboniferous	Xiangshan	1	38,421,062	3,744,778	29.9	106.95	42.24	47.50	123.12	379.27
	Eleventh	2	38,424,402	3,743,841	29.58	106.54	19.71	27.83	101.27	284.96
	Seventh	5	38,430,608	3,736,734	34.11	88.99	13.27	26.16	64.41	289.41
	Tenth	11	38,439,494	3,738,439	400.22	21.77	7.99	91.68	53.01	817.40
	Twelfth	12	38,442,149	3,738,563	88.4	66.42	24.84	112.01	144.86	159.99
	Thirteenth	14	38,442,571	3,750,766	270.67	18.94	8.75	58.86	59.56	584.26
	Shoushan	15	38,445,834	3,743,743	374.22	22.48	13.74	92.47	102.95	809.11
Cambrian	Seventh	5	38,430,608	3,736,734	36.02	64.50	29.11	25.70	62.96	260.88
	Tenth	11	38,439,494	3,738,439	240.56	44.21	30.71	63.93	248.15	432.21
	Twelfth	12	38,442,149	3,738,563	106.90	51.60	25.54	90.37	29.07	392.31
	Eighth	13	38,447,363	3,735,660	133.39	54.98	32.54	56.60	159.14	371.41
	Thirteenth	14	38,442,571	3,750,766	160.08	77.15	40.82	82.6	304.51	335.61
	Shoushan	15	38,445,834	3,743,743	183.08	17.43	18.1	62.39	227.18	197.7

with a total contribution of 99.85 %. Therefore, Na^++K^+, Ca^{2+}, Mg^{2+}, Cl^-, SO_4^{2-}, and HCO_3^- were chosen as the key groundwater chemical components in the Pingdingshan coalfield.

Sampling and analysis

For analysis of groundwater spatial distribution in the Pingdingshan coalfield, the 15 mines were numbered from northwest to southeast (the Xiangshan mine was No. 1, the eleventh mine No. 2, the ninth mine No. 3, the fifth mine No. 4, the seventh mine No. 5, the sixth mine No. 6, the fourth mine No. 7, the third mine No. 8, the first mine No. 9, the second mine No. 10, the tenth mine or Wuzhai mine No. 11, the twelfth mine No. 12, the eighth mine No. 13, the thirteenth mine No. 14, and the Shoushan mine No. 15). Twenty-five samples were collected from the four aquifers in sequence in addition to the original 10 samples, including 6 samples from the Quaternary, 6 samples from the Permian, 7 samples from the Carboniferous, and 6 samples from the Cambrian. Sample analysis results are shown in Table 2.

1. *Comparison of typical characteristics* Key-component distribution curves for the four main aquifers (Fig. 3) were drawn according to the results in Table 2. Groundwater chemical characteristics curves for the four aquifers change significantly between the fifth, seventh, and sixth mines and the twelfth, eighth, and thirteenth mines. Key groundwater chemistry components of the Quaternary and Permian decrease gradually from west to east. A discrepancy in Quaternary groundwater chemical characteristics is obvious between the seventh, sixth and thirteen mines because key groundwater chemical components are significantly affected by the Guodishan fault and the Likou syncline. K^++Na^+ and HCO_3^- concentrations in Permian groundwater change obviously at the seventh and sixth mines, where key groundwater chemical components are significantly affected by the Guodishan fault.

   Key groundwater chemical component concentrations

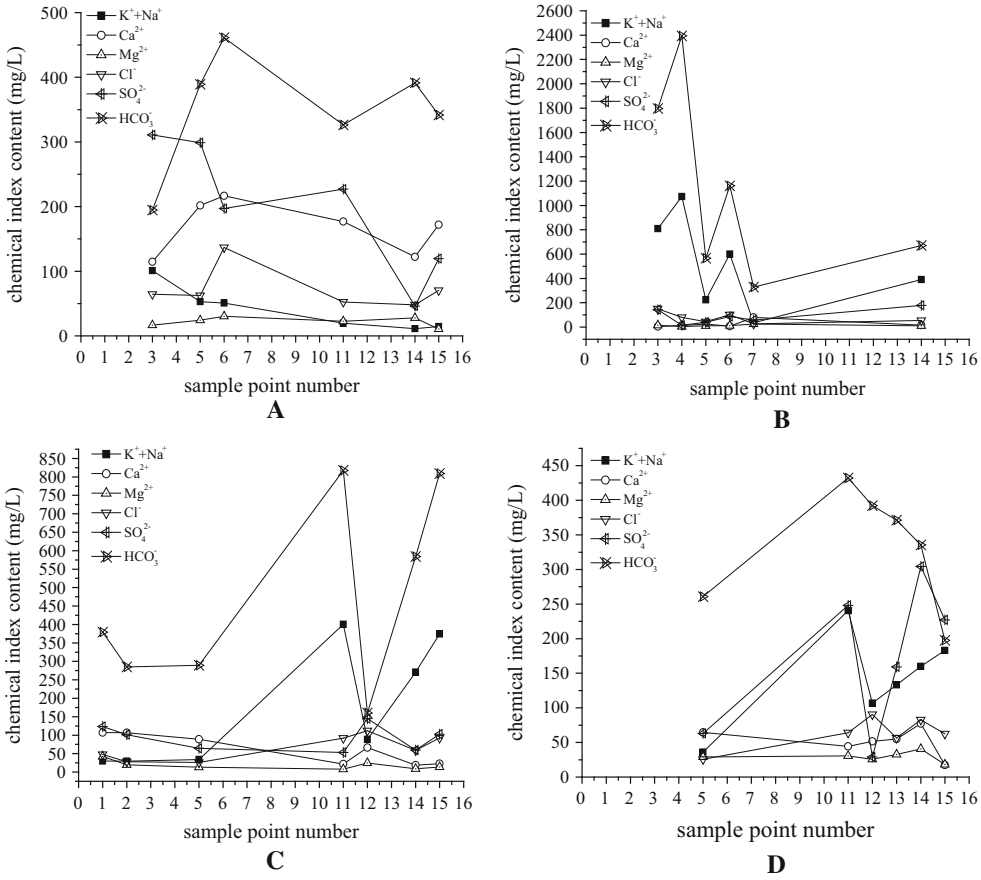

Fig. 3 Key-component spatial distribution *curves* of the four aquifers in the Pingdingshan coalfield. **a** was in the Quaternary, **b** in the Permian, **c** in the Carboniferous, **d** in the Cambrian

in the Carboniferous and Cambrian increase gradually from west to east. Groundwater component concentrations in the Carboniferous changed markedly at the seventh and twelfth mines: K^++Na^+ and HCO_3^- concentrations increased sharply at the seventh mine and decreased markedly at the twelfth mine. Moreover, groundwater component concentrations in the Cambrian increased sharply at the seventh mine, but this trend began to change at the twelfth mine. These results indicated that the Guodishan fault is the primary geological structure affecting key groundwater chemical components in the Carboniferous and Cambrian, with the Likou syncline playing a secondary role.

1. *Spatial distribution characteristics* Contour maps of key groundwater chemical components (Fig. 4) were drawn according to the results in Table 2. The key chemical component contours of the Permian aquifer were similar to those for the Quaternary, gradually declining from west to east in the Pingdingshan coalfield and stabilizing at the sixth mine. These results indicate that the Guodishan fault is the main water-resisting geological structure in the area. Key chemical component contours of the Cambrian aquifer were similar to those of the Carboniferous, with stable trend from west to east in the Pingdingshan coalfield. However, key chemical component contours peaked at the eighth and Shoushan mines because of the Guodishan fault and the Likou syncline.

The analysis described above shows that the groundwater chemical characteristics of the Permian aquifer are similar to those of the Quaternary, that the Guodishan fault is the main water-resisting structure in the area, and that on the two sides of the Likou syncline, groundwater chemical component concentrations are different. The groundwater chemical characteristics of the Cambrian aquifer are similar to those of the Carboniferous, which are more influenced by the Guodishan fault and the Likou syncline.

Results and validation

The Guodishan fault is the primary dividing structure of groundwater chemical characteristics, which divides the Pingdingshan coalfield into two primary groundwater chemically characteristic divisions, I and II. The Likou syncline is a secondary dividing structure for groundwater

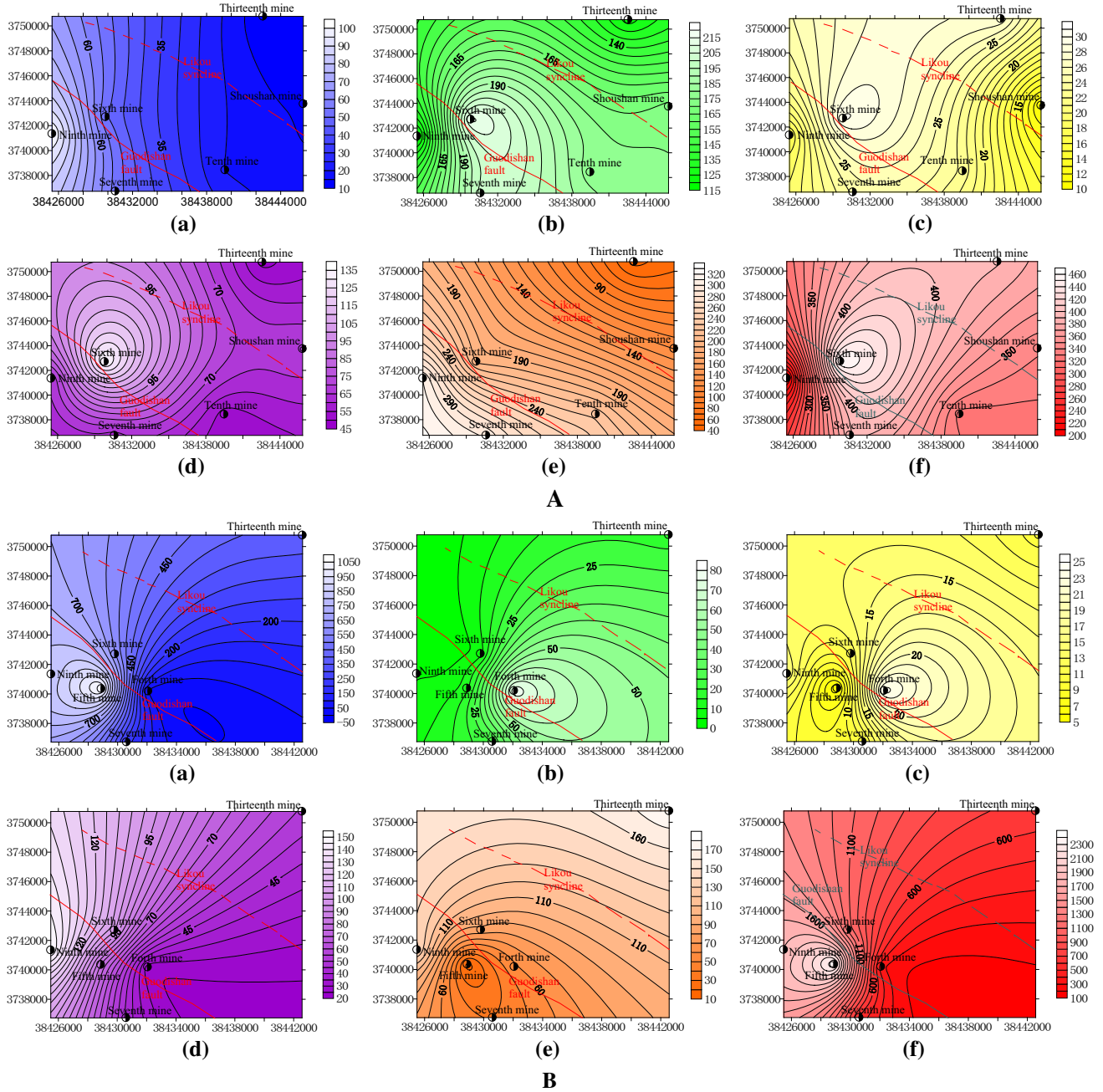

Fig. 4 Contours of key groundwater chemical components in the different aquifers. **A** was in the Quaternary, **B** in the Permian, **C** in the Carboniferous, and **D** in the Cambrian. **a** Showed $K^{+}+Na^{+}$ content, **b** Ca^{2+} content, **c** Mg^{2+} content, **d** Cl^{-} content, **e** $SO_4{}^{2-}$ content, and **f** $HCO_3{}^{-}$ content

chemistry characteristics, which divides II into two secondary groundwater chemically characteristic divisions, II_I and II_{II} (Fig. 5).

Division I occurs to the west of the Guodishan fault, including the fifth, seventh, ninth, Xiangshan, and eleventh mines; division II_I occurs between the Guodishan fault and the Likou syncline, including the first, second, third, fourth, sixth, eighth, tenth, twelfth, and Wuzai mines; and division II_{II} occurs to the east of the Likou syncline, including the Shoushan and thirteenth mines.

The groundwater chemical characteristics of the four aquifers influencing mining operations appeared to have a regional distribution. Discriminant models of groundwater inrush sources in divisions I, II_I, and II_{II} were constructed based on sample data and detailed groundwater chemical

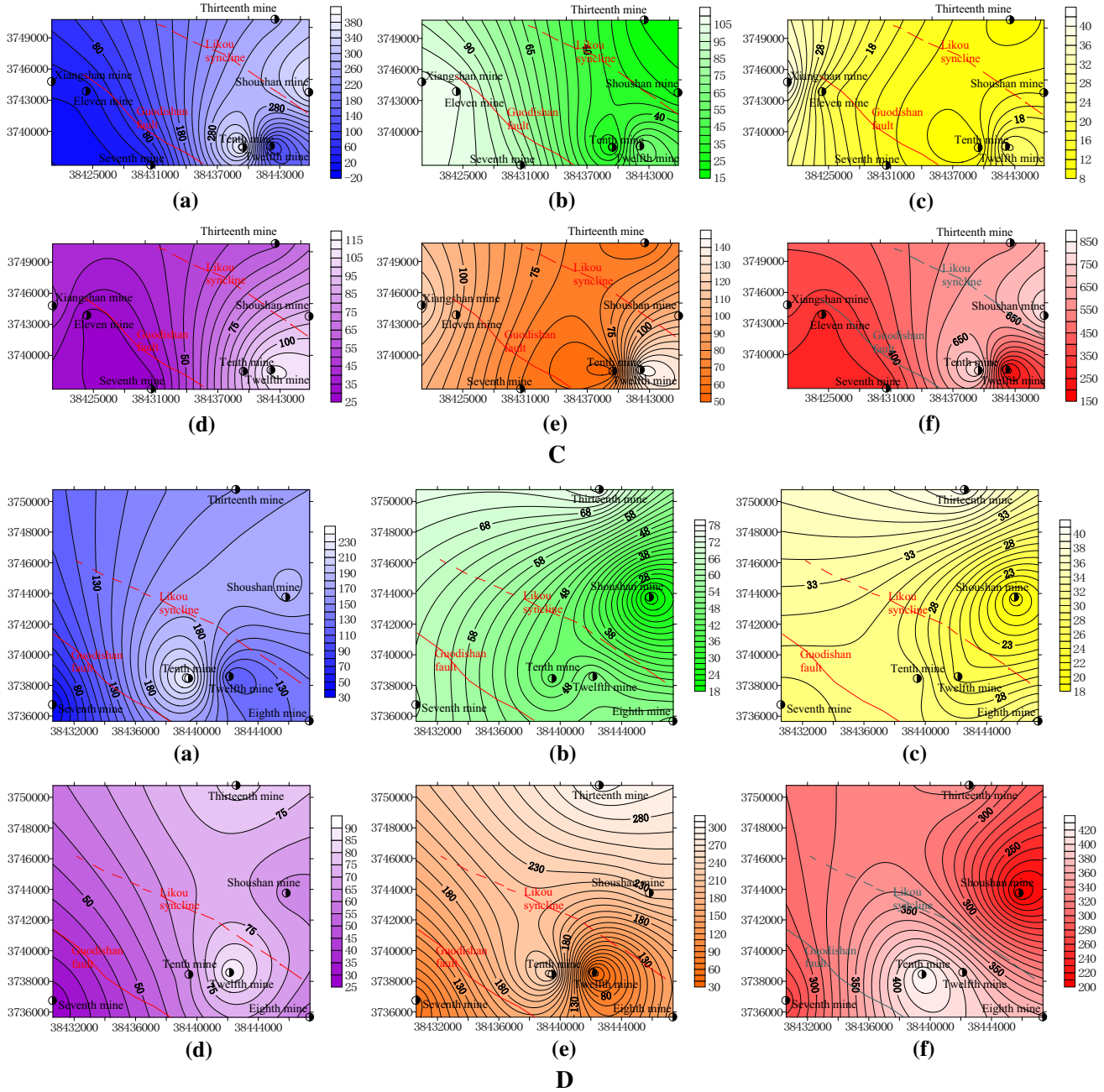

Fig. 4 continued

divisions in the Pingdingshan coalfield, and an engineering verification was conducted.

The discriminant functions were determined according to the Mahalanobis distance (Huang and Chen 2011a, b):

$$y_g(x) = C_{0g} + C_{1g}X_1 + C_{2g}X_2 + \cdots + C_{pg}X_p \quad (1)$$

Take $G = \{x_1, x_2, \cdots, x_m\}^T$ as an m-dimensional population, $X = \{x_1, x_2, \cdots, x_m\}^T$, and suppose that $u_i = E(X_i)(i = 1, 2, \cdots, m)$, so that the overall average vector is $\mu = (\mu_1, \mu_2, \cdots, \mu_m)^T$ and the covariance matrix of population G is $Cov(G) = E[(G - \mu)(G - \mu)^T]$.

The Mahalanobis distance between sample X and population G is defined as:

$$d^2(X, G) = (X - \mu)^T \sum^{-1} (X - \mu) \quad (2)$$

If there are $K(K \geq 2)$ m-dimensional populations and $X = \{x_1, x_2, \cdots, x_m\}^T$ is any given m-dimensional sample,

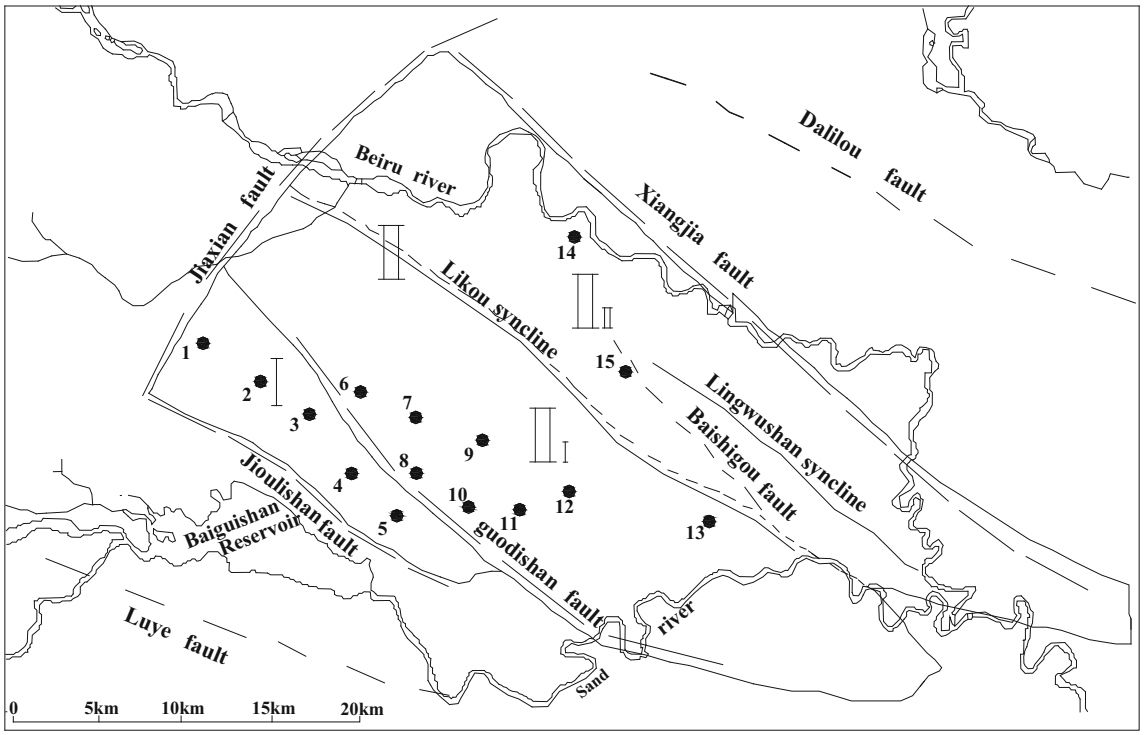

Fig. 5 Groundwater chemical characteristic divisions in the Pingdingshan coalfield. *I* and *II* belong to the primary divisions. II_I and II_{II} belong to the secondary divisions

the sample Mahalanobis distance to every population can be calculated, and then the sample belongs to the minimum population of Mahalanobis distances.

Take the Mahalanobis distance variance of new G_i and G_j samples as:

$$d^2(x, G_1) = \min\{d^2(x, G_i)\} \quad (i = 1, 2, \cdots, m) \tag{3}$$

Therefore, sample $X \in G_i$.

Based on groundwater chemically characteristic divisions I, II_I, and II_{II} in the Pingdingshan coalfield and 36 sample data points for four aquifers in 15 mines (Table 3), the required models were constructed, and the discriminant functions for the Quaternary, Permian, Carboniferous, and Cambrian for the three divisions were denoted as Y_1, Y_2, Y_3, and Y_4.

Division I:

$$Y_1(X) = -103.195 - 0.686X_1 + 1.168X_2 - 2.184X_3 + 0.967X_4 - 0.387X_5 + 0.287X_6$$

$$Y_2(X) = -41.149 - 0.383X_1 + 0.741X_2 - 0.735X_3 + 0.544X_4 - 0.300X_5 + 0.157X_6$$

$$Y_3(X) = -24.529 + 0.379X_1 + 0.326X_2 + 0.541X_3 + 0.204X_4 - 0.083X_5 - 0.159X_6$$

$$Y_4(X) = -36.457 - 0.654X_1 + 0.484X_2 - 1.807X_3 + 0.529X_4 - 0.172X_5 + 0.267X_6$$

Division II_I:

$$Y_1(X) = -90.835 + 0.536X_1 + 1.710X_2 - 0.794X_3 - 0.300X_4 - 0.244X_5 - 0.193X_6$$

$$Y_2(X) = -55.600 - 0.471X_1 - 0.938X_2 + 3.828X_3 + 0.110X_4 + 0.126X_5 + 0.285X_6$$

$$Y_3(X) = -27.124 - 0.280X_1 - 0.521X_2 + 2.203X_3 + 0.148X_4 + 0.089X_5 + 0.169X_6$$

$$Y_4(X) = -98.111 - 1.203X_1 - 2.170X_2 + 5.350X_3 + 0.482X_4 + 0.373X_5 + 0.532X_6$$

Division II_{II}:

$$Y_1(X) = -104.394 + 1.138X_1 + 2.384X_2 + 1.320X_3 + 0.161X_4 - 0.517X_5 - 0.549X_6$$

$$Y_2(X) = -39.389 - 1.195X_1 - 1.612X_2 - 2.704X_3 + 0.921X_4 + 0.674X_5 + 0.558X_6$$

$$Y_3(X) = -13.808 + 0.143X_1 + 0.323X_2 + 0.052X_3 + 0.154X_4 - 0.036X_5 - 0.059X_6$$

$$Y_4(X) = -27.106 - 0.014X_1 + 0.204X_2 - 0.357X_3 + 0.467X_4 + 0.089X_5 - 0.013X_6$$

Six key groundwater chemical components for 16 samples were, respectively, entered into the discriminant the models for divisions I, II_I, and II_{II}. Table 4 shows the

Table 3 Original sample data from the four aquifers

Division	Aquifer	No.	K^++Na^+ (mg/L)	Ca^{2+} (mg/L)	Mg^{2+} (mg/L)	Cl^- (mg/L)	SO_4^{2-} (mg/L)	HCO_3^- (mg/L)
I	Quaternary	1	52.90	201.80	24.18	62.39	298.75	389.31
		2	100.97	114.63	16.65	64.52	310.75	194.65
	Permian	3	809.60	4.80	15.07	151.02	143.12	1796.42
		4	1109.73	15.63	8.88	94.66	24.98	2498.77
		5	1036.85	10.42	1.22	64.17	4.80	2288.25
		6	321.34	3.80	1.38	81.52	21.13	599.42
	Carboniferous	7	90.67	65.99	18.55	36.23	15.06	393.76
		8	54.28	73.80	7.20	8.80	9.30	253.2
		9	12.88	139.28	33.17	38.64	184.92	324.41
		10	39.79	89.58	43.74	44.31	77.33	423.48
		11	41.63	112.02	39.24	40.41	160.9	374.66
	Cambrian	12	30.10	47.42	8.57	29.96	55.02	273.11
		13	39.08	63.93	3.65	17.02	32.51	245.91
II_I	Quaternary	14	50.83	216.83	30.25	136.84	196.92	461.31
		15	19.78	176.95	22.72	52.47	227.18	326.46
	Permian	16	32.89	90.73	24.47	21.86	76.13	352.39
		17	37.49	68.50	24.91	31.80	40.23	303.97
		18	600.28	7.28	12.15	101.82	86.92	1162.06
	Carboniferous	19	88.40	66.42	24.84	112.01	144.86	159.99
		20	513.99	14.56	1.10	101.82	57.94	1074.77
		21	286.44	28.97	14.87	81.54	48.07	560.02
	Cambrian	22	101.02	50.10	30.40	81.46	22.34	420.01
		23	97.66	52.10	26.75	96.73	32.97	361.68
		24	95.33	60.12	25.54	96.73	13.12	408.35
		25	236.07	46.21	31.30	64.38	278.37	432.97
II_{II}	Quaternary	26	6.44	199.40	61.97	124.78	107.59	583.96
		27	14.49	171.94	10.57	70.55	119.59	341.71
	Permian	28	595.38	7.15	10.13	49.63	257.2	985.86
		29	415.92	4.77	5.79	56.72	262.92	583.35
		30	162.08	38.48	15.08	56.03	15.37	444.21
	Carboniferous	31	237.82	29.86	15.07	66.65	113.35	538.81
		32	467.51	18.04	8.51	106.91	102.81	937.62
		33	318.50	22.20	17.90	88.77	20.15	820.30
		34	258.75	37.27	22.6	57.78	202.69	556.5
	Cambrian	35	160.08	77.15	40.82	82.60	304.51	335.61
		36	183.08	17.43	18.10	62.39	227.18	197.70

discrimination results. The discriminant accuracy for the 14 samples was 93.75 %.

Conclusions

1. The key groundwater chemical components of the four aquifers in the Pingdingshan coalfield were Na^++K^+, Ca^{2+}, Mg^{2+}, Cl^-, SO_4^{2-}, and HCO_3^-. Key chemical component concentrations decreased gradually from west to east in Quaternary and Permian aquifers, but increased in Carboniferous and Cambrian aquifers.
2. Key groundwater chemical components in the four aquifers were significantly different on the two sides of the Guodishan fault, which is a major water-resisting structure. Certain differences were also found to exist on the two sides of the Likou syncline, which is a water-conducting structure, over long recharge distances and burial conditions.
3. The Guodishan fault divides the Pingdingshan coalfield into two primary groundwater chemical divisions,

Table 4 Engineering verification results in the Pingdingshan coalfield

Division	No.	X_1 (mg/L)	X_2 (mg/L)	X_3 (mg/L)	X_4 (mg/L)	X_5 (mg/L)	X_6 (mg/L)	Aquifer	Discriminate	Basis
I	1	284.16	13.03	7.05	31.56	4.94	768.84	Permian	Permian	Min adjacent Y_2
	2	68.31	57.72	23.35	18.08	94.14	329.5	Permian	Permian	Min adjacent Y_2
	3	27.37	143.08	19.68	36.16	179.15	314.25	Carboniferous	Carboniferous	Min Y_3
	4	2.69	98.4	6.6	28.4	18.1	268.49	Carboniferous	Carboniferous	Min Y_3
	5	37.03	91.98	49.82	59.56	107.11	389.92	Carboniferous	Carboniferous	Min Y_3
	6	83.72	169.14	36.21	63.46	303.03	423.48	Carboniferous	Carboniferous	Min Y_3
	7	38.87	82.16	18.1	30.13	101.34	263.61	Cambrian	Cambrian	Min Y_4
II_I	8	133.57	44.09	19.46	86.55	47.86	379.18	Cambrian	Cambrian	Min Y_4
	9	246.07	41.21	30.3	63.48	218.37	430.97	Cambrian	Cambrian	Min adjacent Y_4
	10	234.01	48.22	30.92	64.38	277.47	433.91	Cambrian	Cambrian	Min adjacent Y_4
	11	31.51	107.01	30.13	67.00	125.36	286.18	Cambrian	Cambrian	Min Y_4
II_{II}	12	10.28	72.95	10.21	10.99	19.21	241.63	Quaternary	Carboniferous	Min Y_3
	13	452.1	12.4	5.96	116.42	86.16	922	Carboniferous	Carboniferous	Min adjacent Y_3
	14	303.51	8.02	2.43	51.06	5.76	629.7	Carboniferous	Carboniferous	Min adjacent Y_3
	15	179.86	74.75	30.13	63.81	310.27	352.09	Cambrian	Cambrian	Min Y_4
	16	119.83	77.15	36.21	49.98	244.47	338.05	Cambrian	Cambrian	Min Y_4

division I to the west and division II to the east. The Likou syncline divides division II into two secondary groundwater chemical divisions, II_I to the west and II_{II} to the east.

4. Discriminant models of the water inrush sources for the four aquifers were developed based on the three groundwater chemical divisions in the Pingdingshan coalfield and achieved a discrimination accuracy of 93.75 %.
5. The groundwater chemical divisions can be obtained following analysis of the coalfield hydrogeology and water chemical characteristics. The discrimination model of these groundwater chemical divisions can increase the discrimination accuracy of water inrush resources, which can improve the pertinence to and effectiveness on mining inrush water prevention.

Acknowledgments This work was financially supported by the National Natural Science of Foundation of China (Grant 41272250) and Technological Innovation Team of Colleges and Universities in Henan Province of China (Grant 15IRTSTHN027).

References

Alexander YS, Alan M, Sitakanta M (2009) Comparison of deterministic ensemble Kalman filters for assimilating hydrogeological data. Adv Water Resour 32:280–292

Chidambaram S, Anandhan P, Prasanna MV, Srinivasamoorthy K, Vasanthavigar M (2013) Major ion chemistry and identification of hydrogeochemical processes controlling groundwater in and around Neyveli Lignite Mines, Tamil Nadu, South India. Arab J Geosci 6(9):3451–3467

Clemens R, Peter F, Robert GG (2002) Factor analysis applied to regional geochemical data: problems and possibilitie. Appl Geochem 17(3):185–206

Frondini F, Zucchini A, Comodi P (2014) Water-rock interactions and trace elements distribution in dolomite aquifers. Geochem J 48:231–246

Gwo JP, Eduardo FD, Hartmut F, Melanie M, Yeh GT, Phil J (2001) HBGC123D: a high-performance computer model of coupled hydrogeological and biogeochemical processes. Comput Geosci 27:1231–1242

Huang PH, Chen JS (2011a) Fisher indentify and mixing model based on multivariate statistical analysis of mine water inrush sources. J China Coal Soc 36(s1):131–136

Huang PH, Chen JS (2011b) The chemical features of ground water and FDA model used to distinguish source of water burst in Jiaozuo mine area. Coal Geol Explor 39(2):42–51

Huang GX, Sun JC, Chen ZY, Chen X, Jing JH, Liu JT, Zhang YX (2012) Levels and sources of phthalate esters in shallow groundwater and surface water of Dongguan city, South China. Geochem J 46:421–428

Jin PG, Eduardo FDA, Hartmut F (2001) HBGC123D: a high-performance computer model of coupled hydrogeological and biogeochemical processes. Comput Geosci 27:1231–1242

Kuldip S, Harkanwal SH, Dhanwinder S (2011) Geochemistry and assessment of hydrogeochemical processes in groundwater in the southern part of Bathinda district of Punjab, northwest India. Environ Earth Sci 64(7):1823–1833

Lahcen Z, Christian G, Jacky M, Benoit D, Abdel EHZ (2004) Spatial distribution of resistivity in the hydrogeological systems and identification of the catchment area in the Rharb basin. Hydrol Sci J Sci Hydrol 49(3):387–398

Lavoie D, Rivard C, Lefebvre R, Séjourné S, Thériault R, Duchesne MJ, Ahad JME, Wang B, Benoit N, Lamontagne C (2014) The Utica Shale and gas play in southern Quebec: geological and hydrogeological syntheses and methodological approaches to groundwater risk evaluation. Int J Coal Geol 126:77–91

Li QK (2008) Application of gray state synthetic assessment in coalmine water bursting water source differentiation. Coal Geol China 20(7):47–48

Masaoki U, Hikaru I, Hitomi N, Tetsuya Y, Tsuyoshi I, Masaharu T (2014) Elemental transport upon hydration of basic schists during regional metamorphism Geochemical evidence from the Sanbagawa metamorphic belt. Geochem J 48:29–49

Pierre J, Jonny R, Donald V, Julio G, Patrick FD, Mark W, Craig H, Andrea B (2014) A 3D hydrogeological and geomechanical model of an Enhanced Geothermal system at The Geysers. Geothermics 51:240–252

Rajesh R, Brindha K, Murugan R, Elango L (2012) Influence of hydrogeochemical processes on temporal changes in groundwater quality in a part of Nalgonda district, Andhra Pradesh, India. Environ Earth Sci 65(4):1203–1213

Soren J, Flemming L, Dieke P, Pham HV, Nguyen TH, Pham QN, Dang DN, Mai TD, Nguyen TMH, Trieu DH, Tran TL, Dang HH, Rasmus J (2008) Palaeo-hydrogeological control on groundwater As levels in Red River delta, Vietnam. Appl Geochem 23(11):3116–3126

Srinivasamoorthy K, Chidambaram S, Vasanthavigar M, Anandhan P, Sarma VS (2014) Geophysical investigations for groundwater in a hard rock terrain, Salem district, Tamil Nadu, India. Bull Eng Geol Environ Geophys 73(2):357–368

Vittecoq B, Deparis J, Violette S, Jaouën T, Lacquement F (2014) Influence of successive phases of volacnic construction and erosion on Mayotte Island's hydrogeological functioning as determined from a helicopter-borne resistivity survey correlated with borehole geological and permeability data. J Hydrol 509:519–538

Wang GC, Li JS (1992) Groundwater flow systems and karst development in Pingdingshan area. Hydrogeol Eng Geol 4:16–18

Wang XY, Xu T, Huang D (2011) Application of distance discriminance in identifying water inrush resource in similar coalmine. J China Coal Soc 36(8):1354–1358

Wang JS, Wen HJ, Fan HF, Zhu JJ (2012) Sm-Nd geochronology, REE geochemistry and C and O isotope characteristics of calcites and stibnites from the Banian antimony deposit, Guizhou Province, China. Geochem J 46:393–407

Zhou J, Shi XZ, Wang HY (2010) Water-bursting source determination of mine based on distance discriminant analysis model. J China Coal Soc 35(2):278–282

Zhuk EE, Serikova EV (2005) Effectiveness of the step-by-step discriminatory analysis at choosing the informative attributes. Autom Remote Control 66(11):1768–1781